The role of Fis1p–Mdv1p interactions in mitochondrial fission complex assembly

Mary Anne Karren, Emily M. Coonrod, Teresa K. Anderson, and Janet M. Shaw

Department of Biochemistry, University of Utah School of Medicine, Salt Lake City, UT 84132

Mitochondrial division requires coordinated interactions among Fis1p, Mdv1p, and the Dnm1p GTPase, which assemble into fission complexes on the outer mitochondrial membrane. The integral outer membrane protein Fis1p contains a cytoplasmic domain consisting of a tetratricopeptide repeat (TPR)–like fold and a short NH_2-terminal helix. Although it is known that the cytoplasmic domain is necessary for assembly of Mdv1p and Dnm1p into fission complexes, the molecular details of this assembly are not clear. In this study, we provide new evidence that the Fis1p–Mdv1p interaction is direct. Furthermore, we show that conditional mutations in the Fis1p TPR-like domain cause fission complex assembly defects that are suppressed by mutations in the Mdv1p-predicted coiled coil. We also define separable functions for the Fis1p NH_2-terminal arm and TPR-like fold. These studies suggest that the concave binding surface of the Fis1p TPR-like fold interacts with Mdv1p during mitochondrial fission and that Mdv1p facilitates Dnm1p recruitment into functional fission complexes.

Introduction

In most eukaryotic cells, mitochondria form dynamic tubular networks that undergo frequent fusion and fission events. Studies in fungi (Hermann and Shaw, 1998; Yaffe, 1999; Jensen et al., 2000; Shaw and Nunnari, 2002; Westermann, 2002, 2003; Westermann and Prokisch, 2002; Mozdy and Shaw, 2003; Osteryoung and Nunnari, 2003), worms (Labrousse et al., 1999; van der Bliek, 2000), flies (Hales and Fuller, 1997), and mammals (Bossy-Wetzel et al., 2003; Chen and Chan, 2004; Okamoto and Shaw, 2005) indicate that these processes play a critical role in maintaining normal mitochondrial function. In cases where mitochondrial fission is compromised, a variety of defects have been reported. For example, fission is essential for mitochondrial fragmentation and cytochrome *c* release during apoptosis in both worms (Jagasia et al., 2005) and mammalian cell culture (Frank et al., 2001; James et al., 2003; Karbowski and Youle, 2003; Lee et al., 2004). Mitochondrial fission events affect mitochondria–ER interactions important for cellular Ca^{2+} homeostasis and Ca^{2+}-regulated steps in apoptosis (Scorrano, 2003; Szabadkai et al., 2004). A recent study demonstrated that blocking mitochondrial fission limits the maintenance and formation of synapses in cultured neurons, which are processes critical for learning and memory (Li et al., 2004). The latter study raises the possibility that mitochondrial fission defects contribute to a variety of neurodegenerative diseases linked to mitochondrial dysfunction, including Parkinson's disease, Alzheimer's disease, and Huntington's chorea.

Mitochondrial fission has been studied extensively in the budding yeast *Saccharomyces cerevisiae*. Yeast mitochondrial fission requires coordinated interactions between at least three proteins—Fis1p, Dnm1p, and Mdv1p. Fis1p is a tail-anchored outer membrane protein with a tetratricopeptide repeat (TPR)–like domain facing the cytoplasm (Mozdy et al., 2000; Suzuki et al., 2005). Dnm1p is a large GTPase related to mammalian dynamin (Otsuga et al., 1998; Bleazard et al., 1999; Sesaki and Jensen, 1999; Fukushima et al., 2001), and Mdv1p is a WD-repeat protein with an NH_2-terminal extension and a heptad repeat predicted to form a coiled coil (Fekkes et al., 2000; Tieu and Nunnari, 2000; Cerveny et al., 2001). Both Fis1p and Dnm1p have orthologues in many eukaryotic organisms, including worms (Labrousse et al., 1999; Suzuki et al., 2005), plants (Arimura and Tsutsumi, 2002; Suzuki et al., 2005), and humans (Smirnova et al., 1998; James et al., 2003; Yoon et al., 2003). To date, Mdv1p has only been found in fungi.

In yeast cells, punctate structures containing Mdv1p and Dnm1p assemble on the cytoplasmic surface of mitochondrial tubules in a Fis1p-dependent manner (Fekkes et al., 2000; Mozdy et al., 2000; Tieu and Nunnari, 2000; Cerveny et al., 2001).

M.A. Karren and E.M. Coonrod contributed equally to this paper.

Correspondence to Janet M. Shaw: shaw@bioscience.utah.edu

Abbreviations used in this paper: coIP, coimmunoprecipitation; DIC, differential interference contrast; DSP, dithiobis(sulfosuccinimidylpropionate); *fis1-ts*, *fis1* temperature-sensitive mutation; mt-RFP, mitochondrial-targeted red fluorescent protein; pBT, bait plasmid; pTRG, target plasmid; TPR, tetratricopeptide repeat.

The online version of this article contains supplemental material.

The Journal of Cell Biology, Vol. 171, No. 2, October 24, 2005 291–301
http://www.jcb.org/cgi/doi/10.1083/jcb.200506158

These structures, referred to as fission complexes, catalyze mitochondrial division. Only a subset of these complexes are associated with sites that subsequently divide, indicating that assembly and fission are temporally distinct events (Shaw and Nunnari, 2002; Legesse-Miller et al., 2003). Early events include recruitment and assembly of fission complexes, and late events presumably activate processes culminating in membrane scission.

Mdv1p, Dnm1p, and Fis1p interact with each other in vivo, and the domains required for some of these interactions have been mapped (Tieu et al., 2002; Cerveny and Jensen, 2003). However, the order of protein addition into fission complexes and the direct physical contacts required for assembly are unclear. One model suggests that Dnm1p initially assembles onto mitochondria to mark the site of fission and subsequently recruits both Mdv1p and Fis1p to form active fission complexes (Cerveny and Jensen, 2003). A variation of this model postulates that Fis1p-dependent recruitment of Dnm1p occurs first and that addition of Mdv1p remodels and activates the fission complex (Shaw and Nunnari, 2002; Tieu et al., 2002; Osteryoung and Nunnari, 2003). A third possibility is that Fis1p–Mdv1p interactions are a prerequisite for Dnm1p recruitment and assembly. Regardless of the accuracy of these models, Fis1p clearly plays a critical role in assembly because neither Dnm1p nor Mdv1p is recruited to mitochondria in its absence (Shaw and Nunnari, 2002).

The Fis1p cytoplasmic domain contains two distinct structural elements. Structures of mouse (Holm and Sander, 1993), human (Suzuki et al., 2003; Dohm et al., 2004), and yeast Fis1 (Suzuki et al., 2005) proteins reveal that the bulk of the cytoplasmic domain forms a highly conserved TPR-like fold with a concave surface predicted to form a binding interface (D'Andrea and Regan, 2003). The second structural element of the Fis1p cytoplasmic domain is a stretch of residues NH_2-terminal to the TPR-like domain (Suzuki et al., 2003, 2005; Dohm et al., 2004), hereafter referred to as the NH_2-terminal arm. In yeast, the first six residues of the NH_2-terminal arm are flexible, followed by a short helix that binds the concave surface of the TPR-like domain (Suzuki et al., 2005). Multiple functions for this arm have been proposed. One model suggests that the arm facilitates Mdv1p recruitment into fission complexes, and a variation of this model proposes that the arm regulates access to the concave binding surface (Dohm et al., 2004; Suzuki et al., 2005). Both scenarios predict that the Fis1p NH_2-terminal arm and TPR-like domain function independently, although this idea has not been rigorously tested.

To understand the mechanism of Fis1p function, we analyzed Fis1 proteins containing mutations in the TPR-like binding pocket or lacking the NH_2-terminal arm. Our analyses show that Mdv1p binds to the concave surface of the Fis1p TPR-like domain. In support of this idea, mutations exposed at this concave surface are suppressed by mutations in Mdv1p. We provide new evidence that the Fis1p–Mdv1p interaction is direct and define separable functions for the Fis1p NH_2-terminal arm and TPR-like domain at early and late steps during fission. In addition, our results support a revised model in which Dnm1p recruitment into functional fission complexes depends on Fis1p–Mdv1p interactions.

Results

The temperature-sensitive *fis1-3* mutant disrupts mitochondrial fission at 37°C

We hypothesized that the concave TPR-like binding pocket of Fis1p is important for interaction with either Mdv1p or Dnm1p. To test this idea, we isolated *fis1* temperature-sensitive mutations (*fis1-ts;* see Materials and methods) and chose one allele with mutations in the concave surface of the TPR-like domain for further study. This allele (*fis1-3*) encodes three amino acid substitutions (E78D, I85T, and Y88H; Fig. 1 A) that alter semiconserved or conserved residues in helix 4 of the TPR-like domain. Fis1-3p expression and targeting to mitochondria is similar to wild type at both permissive (25°C) and nonpermissive (37°C) temperatures (unpublished data). Individual and pair-wise analyses of each mutation indicate that all three contribute to the temperature-sensitive phenotype of the *fis1-3* allele (unpublished data).

The ability of Fis1-3p to mediate mitochondrial fission was tested by plate phenotype in an *fzo1Δ fis1Δ* strain background. *FZO1* is a gene required for mitochondrial fusion. In *fzo1Δ* strains with a functional copy of Fis1p, mitochondrial fission causes fragmentation, loss of mitochondrial genomes, and a respiratory defect (Hermann et al., 1998; Rapaport et al., 1998). This respiratory defect prevents growth on media containing nonfermentable carbon sources, such as glycerol (Fig. 1 B, top). Blocking fission in *fzo1Δ* cells by mutating *fis1* prevents mitochondrial fragmentation and genome loss, allowing the *fzo1Δ fis1Δ* mutant strains to grow on glycerol (Fig. 1 B, middle). *fzo1Δ fis1Δ* cells expressing Fis1-3p from a plasmid fail to grow on glycerol at 25°C, demonstrating that Fis1-3p mediates fission at this temperature. Growth on glycerol is

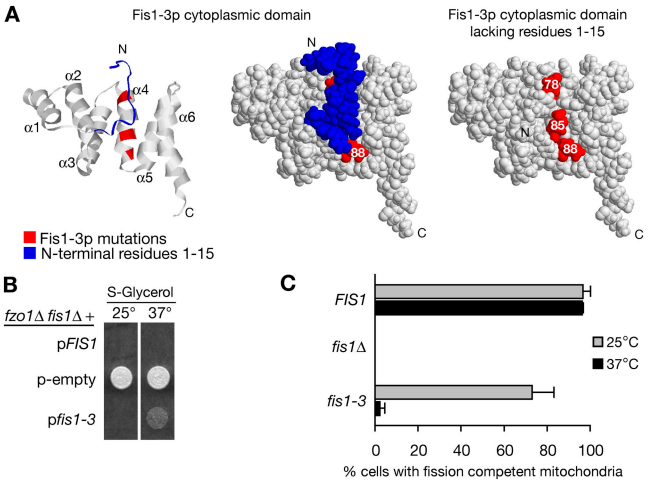

Figure 1. **Mutations in the TPR-like domain of Fis1-3p cause a temperature-sensitive fission defect.** (A) Schematic representations of the yeast Fis1-3p cytoplasmic domain with mutated residues indicated in red and the NH_2-terminal 15 residues in blue. Ribbon diagram shows mutated residues in α-helix 4 of the TPR-like domain (left). Space-fill representations of Fis1-3p showing the position of mutated residues in the concave TPR-like binding pocket are shown with (middle) or without (right) the NH_2-terminal 15 residues. (B) Growth phenotypes of wild-type and fission mutant strains (4×10^3 cells per spot) grown on S-glycerol selective medium at 25 or 37°C. (C) Quantification of mitochondrial morphology in strains grown at 25 or 37°C ($n \geq 300$; SDs are indicated).

partially restored at 37°C, indicating that Fis1-3p is temperature sensitive for mitochondrial fission (Fig. 1 B, bottom).

The *fis1-3* allele was integrated at the *FIS1* locus, and mitochondrial morphology was quantified in log phase cells grown at 25°C or after shifting to 37°C for 2 h. Previous studies showed that fission mutants contain a range of defective mitochondrial morphologies, including a single mitochondrion collapsed to one side of the cell, mitochondrial nets, or mitochondrial tubules lacking branches (Otsuga et al., 1998; Bleazard et al., 1999; Sesaki and Jensen, 1999). By contrast, fission-competent cells contain multiple or branched mitochondrial networks distributed at the cell cortex. In this study, we categorize the latter phenotypic group as "fission competent." When grown at 25 or 37°C, 96% of wild-type cells and 0% of *fis1Δ* cells contain fission-competent mitochondria (Fig. 1 C). *fis1-3* cells, however, displayed 73% fission-competent mitochondria at 25°C versus 2% at 37°C, demonstrating that this allele causes temperature-sensitive mitochondrial morphology defects.

Fis1-3p disrupts mitochondrial fission complex assembly

Fis1-3p could affect assembly of fission complexes or later events that activate fission. To distinguish between these possibilities, we evaluated GFP-tagged Dnm1p or Mdv1p localization in *fis1-3* cells grown at 25°C or shifted to 37°C for 2 h.

In wild-type cells, Dnm1-GFP in fission complexes appears as punctate structures distributed evenly along mitochondrial tubules (Fig. 2 A). At 25°C, ~95% of wild-type and *fis1-3* cells contain Dnm1-GFP puncta that colocalize with mitochondrial tubules. This localization pattern is maintained in *FIS1* wild-type cells shifted to 37°C. Conversely, all visible Dnm1-GFP localizes to the cytoplasm in *fis1-3* cells shifted to 37°C, either in rapidly moving dots or in several randomly localized structures, similar to those in *fis1Δ* cells.

Localization of functional GFP-Mdv1p to mitochondria is also significantly reduced in *fis1-3 mdv1Δ* cells at both temperatures (Fig. 3 A). In wild-type cells, GFP-Mdv1p localizes in punctate fission complexes (Tieu and Nunnari, 2000; Cerveny et al., 2001) and is sometimes also uniformly distributed on mitochondrial tubules (unpublished data). Both localization patterns were scored as punctate GFP-Mdv1p localization in this study. In the majority of *FIS1 mdv1Δ* cells, punctate GFP-Mdv1p colocalizes with mitochondria at both temperatures. However, GFP-Mdv1p puncta on mitochondria are only observed in 49% of *fis1-3 mdv1Δ* cells at 25°C. These puncta are often nearly obscured by cytosolic fluorescence not present in *FIS1* control cells expressing equivalent amounts of GFP-Mdv1p (unpublished data). At 37°C, GFP-Mdv1p localizes almost entirely to the cytoplasm in *fis1-3 mdv1Δ* cells, similar to the GFP-Mdv1p localization pattern in *fis1Δ mdv1Δ* cells. These studies demonstrate that Dnm1-GFP and GFP-Mdv1p do not assemble into mitochondrial fission complexes in *fis1-3* cells at 37°C.

Mdv1^{E250G}p suppresses mitochondrial fission defects in fis1-3 cells

We screened for suppressor mutations in either Dnm1p or Mdv1p that rescued mitochondrial fission defects at 37°C (see Materials and methods). At the time of submission, we had

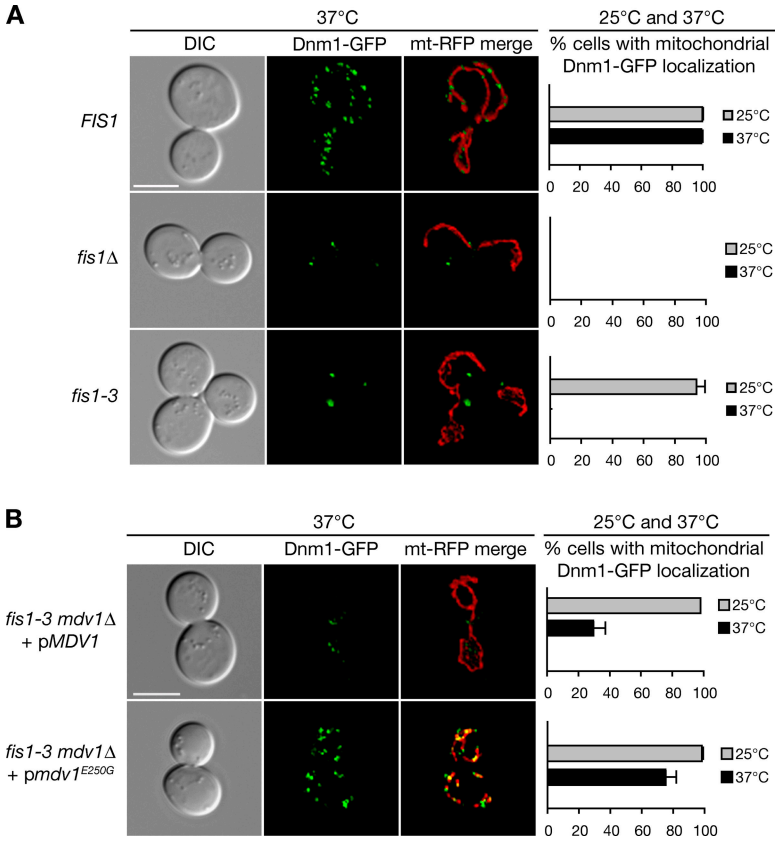

Figure 2. ***fis1-3* mutations cause Dnm1-GFP localization defects that are suppressed by *mdv1*^{E250G}.** DIC (left), Dnm1-GFP (middle), and Dnm1-GFP merged with mt-RFP (right) representative images of indicated strains grown at 37°C are shown. Histograms indicate the percentage of cells with punctate mitochondrial Dnm1-GFP localization at each temperature ($n \geq 300$; SDs are indicated). Genes indicated are genomic unless preceded by "p," which denotes plasmid borne. (A) Dnm1-GFP localization in *FIS1* (top), *fis1Δ* (middle), and *fis1-3* cells (bottom). (B) Dnm1-GFP localization in *fis1-3 mdv1Δ* cells expressing either pRS415*MET25-MDV1* (top) or pRS415*MET25-mdv1*^{E250G} (bottom). Bars, 5 μm.

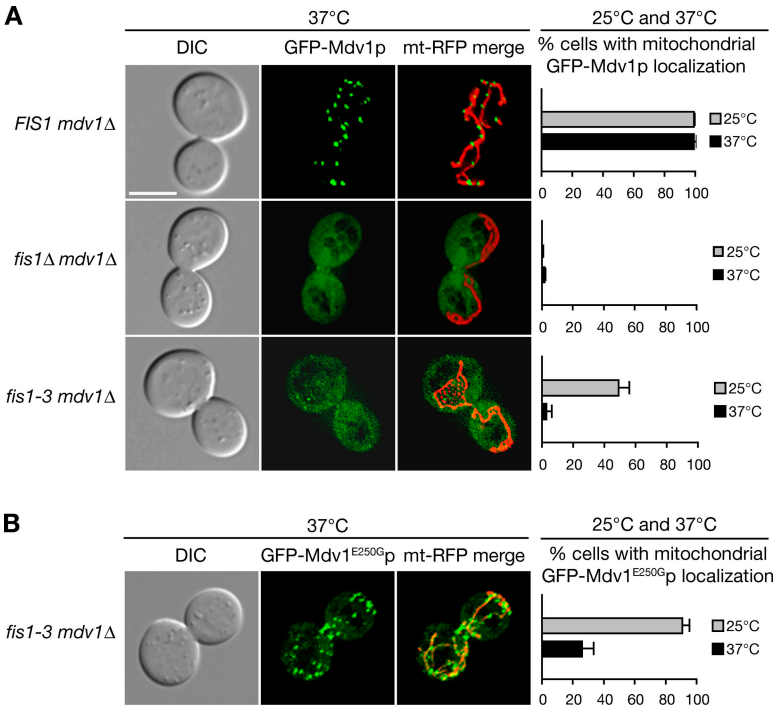

Figure 3. ***fis1-3* mutations cause GFP-Mdv1p localization defects that are suppressed by the E250G substitution.** DIC (left), GFP-Mdv1p or GFP-Mdv1^{E250G}p (middle), and GFP-Mdv1p or GFP-Mdv1^{E250G}p merged with mt-RFP (right) images of indicated strains grown at 37°C are shown. Histograms indicate the percentage of cells with mitochondrial localization of GFP-Mdv1p or GFP-Mdv1^{E250G}p at each temperature ($n \geq 300$; SDs are indicated). (A) GFP-Mdv1p localization in *FIS1 mdv1Δ* (top), *fis1Δ mdv1Δ* (middle), and *fis1-3 mdv1Δ* cells (bottom). (B) GFP-Mdv1^{E250G}p localization in *fis1-3 mdv1Δ* cells. To maximize visibility of GFP-Mdv1p, we used *mdv1Δ* cells expressing plasmid-borne GFP-Mdv1p from the *MET25* promoter without induction. Bar, 5 μm.

identified no *dnm1* alleles that suppressed *fis1-3* phenotypes. However, we identified several robust suppressor alleles that altered residues in *MDV1*. These suppressor mutations are located in or immediately upstream of the *MDV1* predicted coiled-coil–forming domain. One of these, *mdv1^{E250G}* (Fig. 4 A), was characterized in detail.

A glycerol growth assay with the *fzo1-1* strain indicates that Mdv1^{E250G}p restores mitochondrial fission in *fis1-3* cells at 37°C. In temperature-sensitive *fzo1-1* cells, ongoing mitochondrial fission causes fragmentation, mitochondrial genome loss, and inability to grow on glycerol medium at 37°C (Fig. 4 B, top; Hermann et al., 1998). Disrupting fission in this strain by introducing *fis1-3* mutations prevents mitochondrial fragmentation and genome loss, allowing *fzo1-1 fis1-3* strains to grow on glycerol at the elevated temperature. Expression of wild-type Mdv1p from a plasmid does not restore the temperature-sensitive glycerol growth defect in this strain (Fig. 4 B, middle). By contrast, *fzo1-1 fis1-3* cells expressing Mdv1^{E250G}p from a plasmid fail to grow on glycerol at 37°C (Fig. 4 B, bottom), indicating that Mdv1^{E250G}p restores mitochondrial fission.

The effect of Mdv1^{E250G}p on *fis1-3* mitochondrial morphology was compared in cells expressing either wild-type Mdv1p or Mdv1^{E250G}p from the inducible *MET25* promoter. Although the suppressors were isolated by plate phenotype without induction of the *MET25* promoter, suppression of mitochondrial morphology defects was optimal in log phase cultures after induction for 2 h in medium lacking methionine. Under these conditions, mitochondria in 70% of *fis1-3 mdv1Δ* cells incubated at 37°C and expressing Mdv1^{E250G}p are tubular and branched, with multiple mitochondria per cell (Fig. 4 C). By contrast, <10% of *fis1-3 mdv1Δ* cells expressing equivalent amounts of wild-type Mdv1p have fission-competent mitochondria.

Mdv1^{E250G}p rescues fission phenotypes in *mdv1Δ* cells and behaves like wild-type Mdv1p under all other conditions tested (Fig. S1, available at http://www.jcb.org/cgi/content/full/jcb.200506158/DC1). Thus, the effects of the Mdv1^{E250G} suppressor protein are only apparent in *fis1* mutant cells.

Mdv1^{E250G}p suppresses mitochondrial fission complex assembly defects in *fis1-3* cells

Localization experiments confirm that fission complex assembly is restored in *fis1-3* cells expressing Mdv1^{E250G}p. After induction of Mdv1^{E250G}p from the *MET25* promoter in the *fis1-3 mdv1Δ* strain at 37°C, Dnm1-GFP assembles into fission complexes on mitochondria in 75% of cells (Fig. 2 B, bottom). Interestingly, overexpression of wild-type Mdv1p also allows Dnm1-GFP to assemble into punctate structures in 30% of the population at 37°C (Fig. 2 B, top). However, mitochondrial fission is not significantly rescued in these cells (Fig. 4 C). Thus, although Dnm1p can be recruited to Fis1-3p–containing mitochondria by overexpressed Mdv1p, this Dnm1p localization is not sufficient to mediate mitochondrial fission. Instead, restoration of mitochondrial fission in *fis1-3* cells requires the Mdv1^{E250G} suppressor protein.

Analysis of GFP-Mdv1^{E250G}p localization in *fis1-3 mdv1Δ* cells demonstrates that the E250G substitution enhances Mdv1p recruitment to Fis1-3p–containing mitochondria. At 25°C, GFP-Mdv1^{E250G}p localizes to punctate structures on mitochondria in 91% of cells, a 40% increase in localization compared with wild-type GFP-Mdv1p. After shifting to 37°C for 2 h, GFP-Mdv1^{E250G}p continues to localize to mitochondria in 26% of the population as compared with 3% of GFP-Mdv1p–expressing cells. These results demonstrate that GFP-Mdv1^{E250G}p localizes more efficiently to Fis1-3p–containing mitochondria than GFP-Mdv1p.

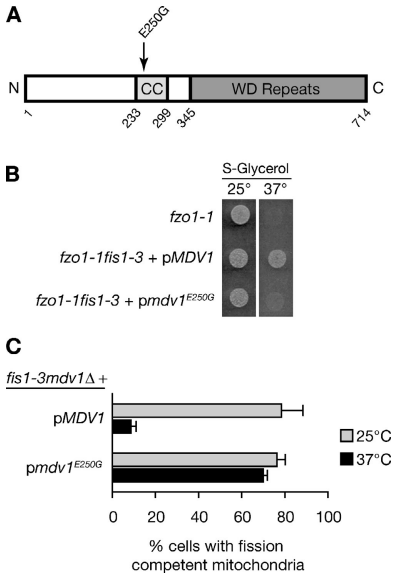

Figure 4. **The Mdv1^{E250G}p mutation suppresses the temperature-sensitive Fis1-3p fission defect.** (A) Schematic representation of Mdv1p, with the positions of the predicted coiled coil (CC), WD-repeat region, and E250G substitution indicated. (B) Growth phenotypes of indicated strains (800 cells per spot) grown on S-glycerol selective media at either 25 or 37°C. Fission is disrupted (indicated by growth) at 37°C in *fzo1-1 fis1-3* cells expressing plasmid-borne Mdv1p (middle). Fission is restored (indicated by no growth) at 37°C in *fzo1-1 fis1-3* cells expressing plasmid-borne Mdv1^{E250G}p (bottom), similar to *fzo1-1* cells (top). (C) Quantification of mitochondrial morphology ($n \geq 300$, SDs are indicated) in strains grown at 25 or 37°C.

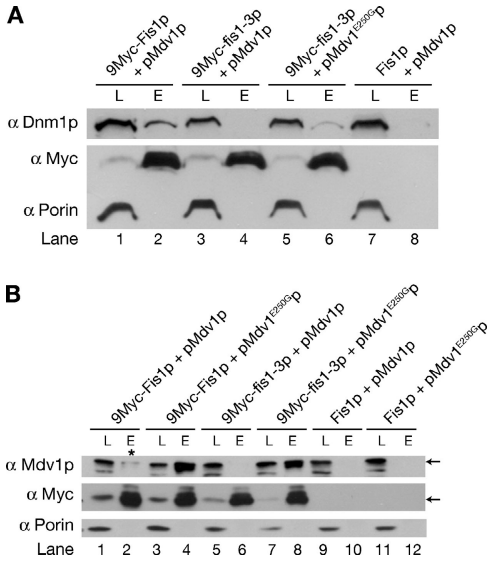

Figure 5. **Fis1p physical interactions are disrupted by *fis1-3* mutations and rescued by Mdv1^{E250G}p.** CoIP experiments demonstrating interactions between Fis1 proteins and Dnm1p or Mdv1 proteins. Fis1 proteins were immunoprecipitated using anti-Myc agarose-conjugated beads. CoIP of Dnm1p or Mdv1 proteins was detected with either native Dnm1p or Mdv1p antibodies (top). Western blots show total loaded (L) and eluted (E) proteins. Immunoprecipitation of 9Myc-Fis1p or 9Myc–Fis1-3p was detected with anti–c-Myc antibodies (middle). The mitochondrial protein porin is provided as a loading control (bottom). (A) Fis1 and Dnm1 proteins coimmunoprecipitated from DSP–cross-linked yeast spheroplasts. (B) Fis1 and Mdv1 proteins coimmunoprecipitated from whole cell lysates in the absence of cross-linking. Asterisk shows that wild-type Mdv1p reproducibly coimmunoprecipitated with wild-type Fis1p at lower levels than Mdv1^{E250G}p. Arrows denote full-length proteins.

Fis1-3p interaction defects are suppressed by Mdv1^{E250G}p

In vivo localization experiments show that Fis1-3p abolishes recruitment of both Mdv1p and Dnm1p to mitochondria at 37°C and that Mdv1^{E250G}p suppresses these defects. As a complementary approach, we used coimmunoprecipitation (coIP) assays to analyze the physical interaction between wild-type or mutant Fis1 proteins with either Dnm1p or Mdv1p. We also tested the effect of the Mdv1^{E250G}p suppressor on these interactions.

Previous attempts to coimmunoprecipitate Fis1p and Dnm1p from yeast have been unsuccessful, possibly because Dnm1p-containing structures are easily dissociated from Fis1p and mitochondria during cell solubilization. To prevent this dissociation, we spheroplasted cells expressing wild-type 9Myc-Fis1p or mutant 9Myc–Fis1-3p and treated with a cross-linking reagent, dithiobis(sulfosuccinimidylpropionate) (DSP), before homogenization. After immunoprecipitation with anti-Myc agarose-conjugated beads, the eluted protein fractions were assayed by immunoblotting with Dnm1p-specific antibodies.

9Myc-Fis1p and 9Myc–Fis1-3p are efficiently immunoprecipitated from DSP-treated cells (Fig. 5 A, anti-Myc, lanes 2, 4, and 6), and a fraction of cellular Dnm1p reproducibly coimmunoprecipitates with 9Myc-Fis1p (Fig. 5 A, anti-Dnm1p, lane 2). Neither Fis1p nor Dnm1p immunoprecipitates when Fis1p lacks the 9Myc tag (Fig. 5 A, anti-Dnm1p and anti-Myc, lane 8), indicating that the precipitation is antibody dependent. Significantly, Dnm1p does not coimmunoprecipitate with 9Myc–Fis1-3p when wild-type Mdv1p is expressed (Fig. 5 A, anti-Dnm1p, lane 4), confirming that the Fis1-3p mutations disrupt Dnm1p–Fis1p complex formation. Expression of Mdv1^{E250G}p rather than Mdv1p increases the amount of Dnm1p recovered with 9Myc–Fis1-3p (Fig. 5 A, anti-Dnm1p, lane 6), although not to wild-type levels. Together, the in vivo localization and coIP experiments demonstrate that Mdv1^{E250G}p partially restores Dnm1p association with Fis1-3p in mitochondrial fission complexes.

CoIP assays to test the Fis1-3p physical interaction with Mdv1p were performed from solubilized cells (without cross-linking) expressing 9Myc-Fis1p or 9Myc–Fis1-3p. Proteins were immunoprecipitated with anti-Myc–conjugated beads, and eluted proteins were analyzed by Western blotting with Mdv1p-specific antibodies. Both 9Myc-Fis1p and 9Myc–Fis1-3p are efficiently immunoprecipitated from cell lysates (Fig. 5 B, anti-Myc, lanes 2, 4, 6, and 8). As reported previously, Mdv1p coimmunoprecipitates with 9Myc-Fis1p (Fig. 5 B, anti-Mdv1p, lane 2; Tieu et al., 2002) in an antibody-dependent manner (Fig. 5 B, anti-Mdv1p and anti-Myc, lanes 10 and 12). However, Mdv1p does not coimmunoprecipitate appreciably with 9Myc–Fis1-3p (Fig. 5 B, anti-Mdv1p, lane 6). This result confirms that the Fis1-3p mutations disrupt physical interactions with Mdv1p. When Mdv1^{E250G}p rather than Mdv1p is expressed, significantly more Mdv1^{E250G}p coimmunoprecipitates with both 9Myc-Fis1p and 9Myc–Fis1-3p (Fig. 5 B, anti-Mdv1p, lanes 4 and 8). This result demonstrates that cellular Mdv1^{E250G}p interacts with Fis1 proteins more efficiently than wild-type Mdv1p.

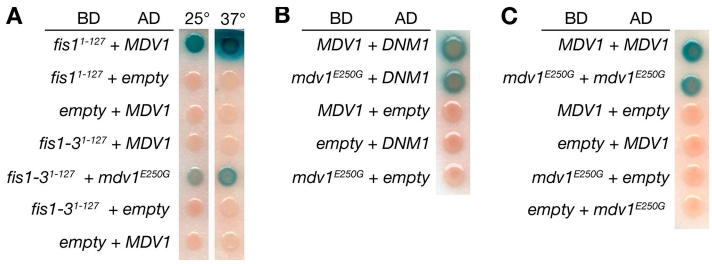

Figure 6. **The Mdv1^{E250G}p suppressor specifically affects interactions with Fis1-3p.** Yeast two-hybrid assays show interactions between Mdv1 and Fis1 proteins (A), between Mdv1 proteins and Dnm1p (B), and between Mdv1 proteins (C). pBD and pAD plasmids carrying the indicated genes were cotransformed into the Y187 yeast two-hybrid reporter strain. Strains were grown on S-dextrose selective plates at 25°C, and a filter lift β-galactosidase assay was performed at either 25 or 37°C (A) or at 25°C (B and C). Blue indicates positive interaction. Mdv1^{E250G}p also interacts with Fis1$^{1–127}$p in this assay (unpublished data).

The Mdv1 E250G substitution primarily affects interactions between Mdv1p and Fis1p

Mdv1p can interact with Fis1p, with Dnm1p, and with itself (Tieu et al., 2002; Cerveny and Jensen, 2003). The E250G substitution might stabilize fission complex assembly and suppress *fis1-3* phenotypes by affecting one or more of these binding partner interactions. We were unable to purify soluble forms of Mdv1p or Mdv1^{E250G}p to quantitatively measure relative binding affinities in vitro. Instead, we used a two-hybrid approach to determine qualitatively which Mdv1 protein interactions are most affected by the E250G substitution.

As published previously (Tieu et al., 2002; Cerveny and Jensen, 2003), Mdv1p fused to the Gal4 activating domain (AD-Mdv1p) interacts with the Fis1p cytoplasmic domain fused to the Gal4 DNA-binding domain (BD-Fis1$^{1–127}$p) to stimulate transcription of *GAL4* reporter genes (Fig. 6 A). Although AD-Mdv1p fails to interact with the mutant BD–Fis1-3$^{1–127}$p, the suppressor AD-Mdv1^{E250G}p interacts robustly with BD–Fis1-3$^{1–127}$p. Introducing the E250G mutation does not affect interaction of Mdv1p with Dnm1p (Fig. 6 B) or with itself (Fig. 6 C) in this assay. In control experiments, constructs paired with empty vectors did not activate transcription. These results are consistent with the idea that the E250G mutation primarily affects heterotypic interactions of Mdv1p with Fis1p, rather than with Dnm1p or with itself. In combination with our coIP experiments, these studies suggest that suppression of Fis1-3p by Mdv1^{E250G}p is primarily the result of increased interaction between Mdv1 and Fis1 proteins.

Fis1p interacts directly with Mdv1p

A mechanistic understanding of *fis1-3* suppression by Mdv1^{E250G}p requires precise knowledge of how the wild-type proteins interact. To date, all experiments evaluating Fis1p–Mdv1p interactions have been performed under conditions where other yeast proteins are present (Tieu et al., 2002; Cerveny and Jensen, 2003). Therefore, these experiments do not determine whether Fis1p–Mdv1p interactions are direct or bridged by other yeast proteins. To address this issue, we performed a two-hybrid assay in bacterial cells (Fig. 7). The *fis1* cytoplasmic domain (amino acids 1–127) and full-length *MDV1* were cloned into bait plasmids (pBTs) and target plasmids (pTRGs), respectively, and expressed in bacteria. A positive interaction in this assay stimulates transcription of bacterial *HIS3*. This expression allows cells to grow in histidine-limiting conditions in the presence of 3AT (3-amino-1,2,4-triazole), a competitive inhibitor of the *HIS3* gene product. In serial dilution experiments, cells cotransformed with pBT-*fis1*$^{1–127}$(encoding amino acids 1–127) and pTRG-*MDV1* grow significantly better on medium lacking histidine and containing 3AT than cells containing either construct alone. This experiment establishes for the first time that the Fis1p–Mdv1p interaction requires no additional yeast proteins.

Purified Fis1-3p is more susceptible to proteolytic cleavage than wild-type Fis1p

Fis1-3p mutations lie on the concave surface of the TPR-like fold. These substitutions could affect a specific binding surface without compromising the overall protein fold, or the mutations could cause global folding changes. To distinguish between these possibilities, limited proteolysis was performed on the purified cytoplasmic domains of Fis1p and Fis1-3p (amino acids 1–127 fused to 10His at the COOH terminus).

Western blot analysis shows that wild-type Fis1$^{1–127}$10Hisp is extremely resistant to trypsin digestion, with uncut protein persisting at high protease concentrations (Fig. 8, top panel, top band). Digestion with increasing trypsin concentration converts this full-length protein to a stable, lower molecular weight band (Fig. 8, top panel, bottom band). Mass spectrometry of digested samples reveals a mixture of several proteolytic fragments generated predominantly by cleavage at the NH_2 and COOH termini (unpublished data). NH_2-terminal cleavage sites occur in the first five residues, consistent with nuclear magnetic resonance studies showing that the NH_2-terminal five residues of yeast Fis1p are unstructured (Suzuki et al., 2005). COOH-terminal cleavage sites are located throughout the 10His tag used for purification. Importantly, fragments generated by cleavage at sites internal to the protein are rarely observed. Thus, the TPR-like domain and NH_2-terminal helix form a highly stable fold, with the most labile portion at the extreme NH_2 terminus.

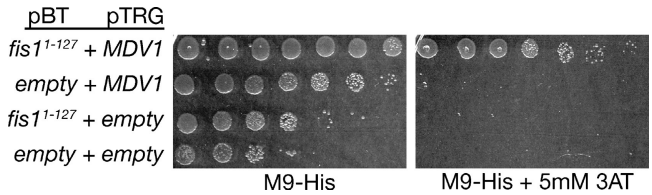

Figure 7. **Fis1p and Mdv1p interact in the absence of other yeast proteins.** pBT and pTRG plasmids carrying the indicated genes were cotransformed into an *E. coli* two-hybrid reporter strain. Cells were grown at 30°C on M9 medium lacking histidine in the presence or absence of 5 mM 3AT. Growth on M9 − His + 5 mM 3AT indicates a positive interaction.

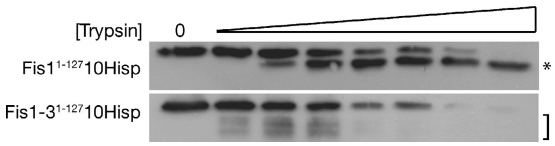

Figure 8. **Fis1-3p is more sensitive to protease than wild-type Fis1p.** Limited proteolysis of the wild-type Fis1$^{1-127}$10Hisp (top) and mutant Fis1-3$^{1-127}$10Hisp (bottom). Purified proteins were digested with 0, 0.1, 0.5, 1, 2, 3, 4, or 5 μg of trypsin in a 10-μl reaction vol (see Materials and methods). Digestion was performed at 37°C for 2 min, and samples were analyzed by Western blot using anti-Fis1p antibody. Bracket marks proteolytic fragments. Asterisk marks species lacking 10His tag.

By contrast, trypsin sites in the mutant Fis1-3$^{1-127}$10Hisp are more accessible to protease. As observed with wild type, the higher molecular weight band (consisting of uncut protein) persists at high trypsin concentrations (Fig. 8, bottom panel, top band). However, digestion of the mutant protein yields multiple lower molecular weight products that are rapidly degraded as trypsin concentration increases (Fig. 8, bottom panel, bracket). Mass spectrometry confirms that trypsin digestion of the mutant protein does not produce the same stable lower molecular weight species as digestion of wild type (unpublished data). Instead, minor species contain cut sites at both the NH_2 and COOH termini and at random sites within the TPR-like fold. The presence of uncut protein in digested samples suggests that the mutant protein folds in vitro. However, the structure is clearly more labile in solution than the wild-type protein.

Mitochondrial fission complex assembly and fission can occur without the Fis1p NH_2-terminal arm

To further define the functions of the Fis1p NH_2-terminal arm and TPR-like domain, we evaluated mitochondrial morphology and fission complex assembly in cells expressing a Fis1 mutant lacking the NH_2-terminal arm (Fis1$^{15-155}$p). Fis1$^{15-155}$p alone or Fis1$^{15-155}$p and either Mdv1p or Mdv1^{E250G}p were expressed under control of the inducible *MET25* promoter using a 30-min induction period, and mitochondrial morphology was quantified. Consistent with a previous study (Suzuki et al., 2005), <10% of *fis1Δ* cells expressing Fis1$^{15-155}$p and endogenous Mdv1p have fission-competent mitochondria (Fig. 9 A). However, when both Fis1$^{15-155}$p and Mdv1p are simultaneously induced from *MET25* promoters in *fis1Δ mdv1Δ* cells, 45% of cells contain fission-competent mitochondria. In control experiments, 58% of *fis1Δ mdv1Δ* cells expressing wild-type Fis1p and Mdv1p contain fission-competent mitochondria. Interestingly, Mdv1^{E250G}p and Mdv1p rescue mitochondrial fission defects to the same extent in this experiment (unpublished data).

We also evaluated the effect of the NH_2-terminal arm truncation on localization of GFP-tagged Dnm1p and Mdv1p in cells expressing Fis1$^{15-155}$p. Dnm1-GFP localizes to mitochondria in 44% of *fis1Δ* cells (44.1% ± 15.0 localized, $n = 600$) expressing high levels of Fis1$^{15-155}$p and endogenous Mdv1p but localizes to mitochondria in 75% of cells after a 30-min induction of both Fis1$^{15-155}$p and Mdv1p (75.2 ± 6.14 localized, $n = 500$). Thus, Dnm1-GFP localization is reduced in *fis1$^{15-155}$* cells, and this defect is rescued by Mdv1p overexpression.

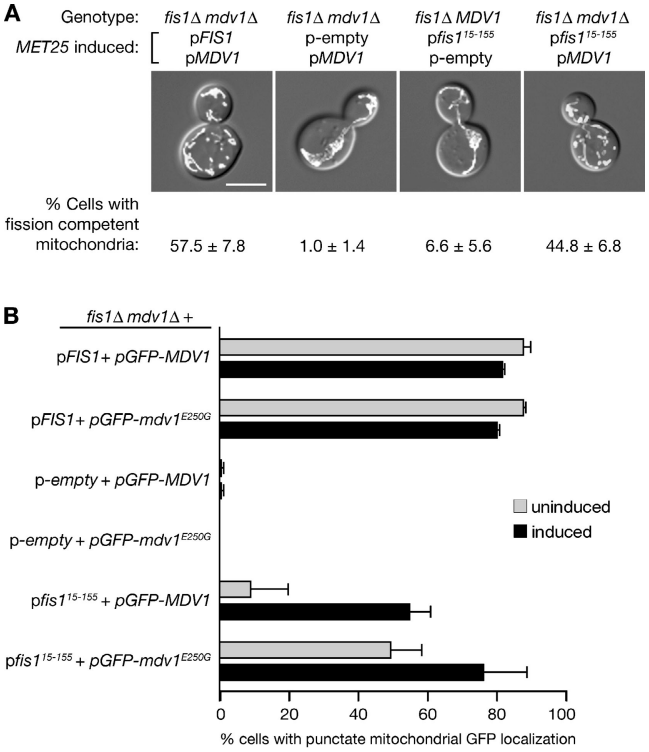

Figure 9. **Mitochondrial fission can occur in the absence of the Fis1p NH_2-terminal arm.** (A) Mitochondrial morphology in cells expressing Fis1$^{15-155}$p and Mdv1p from the *MET25* promoter. Panels contain superimposed DIC and mt-RFP images representative of phenotypes observed at 25°C. The percentage of cells in the population with fission-competent mitochondria is shown below each panel ($n \geq 300$; ± indicates SD). Bar, 5 μm. (B) Quantification of GFP-Mdv1p or GFP-Mdv1^{E250G}p localization with (black bars) or without (gray bars) *MET25* induction (30 min). Genes indicated are genomic unless preceded by "p," which denotes plasmid borne under the control of the *MET25* promoter ($n \geq 300$; SDs are indicated).

When low levels of Fis1$^{15-155}$p and GFP-Mdv1p are expressed in *fis1Δ mdv1Δ* cells, GFP-Mdv1p colocalizes with mitochondria in <10% of cells (Fig. 9 B). However, GFP-Mdv1p colocalizes with mitochondria in ~55% of these cells after induction of both Fis1$^{15-155}$p and GFP-Mdv1p. Interestingly, GFP-Mdv1^{E250G}p localizes to mitochondria significantly better than GFP-Mdv1p in these cells, both under low (49% localized) and high (76% localized) expression conditions. This result indicates that interactions between Mdv1p and the TPR-like domain of Fis1p are enhanced by the Mdv1 E250G substitution.

These combined observations suggest that the NH_2-terminal arm facilitates, but is not strictly required for, Mdv1p recruitment or stabilization of fission complexes. Moreover, the Fis1p TPR-like domain lacking the NH_2-terminal arm is sufficient to mediate fission complex assembly and fission under specific conditions.

Discussion

The experiments described here make three main advances. First, we define early and late functions for the Fis1p NH_2 terminus and TPR-like domain. Second, our data demonstrate that Fis1p and Mdv1p interact directly and strongly suggest that

this interaction occurs via the concave surface of the TPR-like domain. Third, our experiments support a revision of current models for fission complex assembly. In the following sections, we discuss each of these issues in detail.

Separable functions of the Fis1p NH_2-terminal arm and TPR-like domain

In this study, we sought to relate the structure of Fis1p to its molecular role in fission. Fis1p contains three distinctive features: a COOH-terminal transmembrane domain, an NH_2-terminal arm, and a six-helix TPR-like domain with a hydrophobic pocket on its concave surface. In yeast, a short helical portion of the NH_2-terminal arm occupies the hydrophobic pocket. The structure of the TPR-like fold, and presumably its function, is highly conserved among orthologues (Suzuki et al., 2003, 2005; Dohm et al., 2004). However, the length, conservation, and placement of the NH_2-terminal arms differ (Mozdy et al., 2000; James et al., 2003; Yoon et al., 2003; Dohm et al., 2004; Stojanovski et al., 2004), suggesting that this region has acquired a function distinct from that of the TPR-like fold.

We provide evidence that the NH_2-terminal arm acts early, during complex assembly. Consistent with a previous study (Suzuki et al., 2005), removal of the Fis1p NH_2-terminal arm disrupts Mdv1p and Dnm1p recruitment into fission complexes. Thus, the NH_2-terminal arm is important for an early assembly step. However, in the absence of the NH_2-terminal arm, fission complex assembly and fission are rescued by overexpression of Mdv1p. Therefore, the NH_2-terminal arm is not essential after assembly, and the TPR-like domain is sufficient for fission events once assembly has occurred.

Characterization of the Fis1p–Mdv1p interaction

To date, all experiments evaluating Fis1p–Mdv1p interactions have been performed in live cells (yeast two-hybrid assay and genetic studies) or extracts (coIP) containing other yeast proteins. Here we use an *Escherichia coli* two-hybrid assay to demonstrate that Fis1p and Mdv1p interact directly in the absence of other yeast proteins.

Is the Mdv1p-binding site on yeast Fis1p formed by the NH_2-terminal arm, the TPR-like domain, or both? It has been hypothesized that the TPR-like hydrophobic pocket is a binding surface for other fission complex proteins (Dohm et al., 2004; Suzuki et al., 2005). Three lines of evidence that are presented in this study support the idea that Mdv1p occupies the Fis1p TPR-like binding pocket, possibly by displacing the NH_2-terminal arm (Fig. 10). First, mutations in the Fis1p TPR-like binding pocket are suppressed by mutations in Mdv1p. Second, overexpressed Mdv1p interacts with $Fis1^{15–155}$p, which lacks the NH_2-terminal arm. Third, the $Mdv1^{E250G}$p suppressor interacts with $Fis1^{15–155}$p, even when expressed at low levels. Thus, the TPR-like domain alone interacts with Mdv1p, and this interaction is augmented by the Mdv1p E250G substitution. Although these studies establish that Mdv1p interacts with the TPR-like domain, the Fis1p NH_2-terminal arm is clearly important. We propose that the Fis1p NH_2-terminal arm facilitates recruitment and/or stabilization of Mdv1p during fission complex assembly.

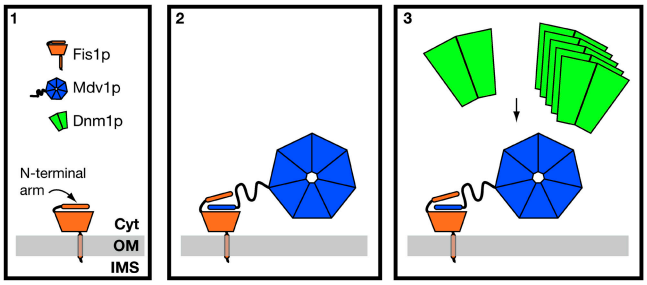

Figure 10. **Proposed pathway for mitochondrial fission complex assembly.** (1) Before fission complex assembly, the NH_2-terminal arm of yeast Fis1p (indicated) interacts with the TPR-like binding pocket (Suzuki et al., 2005). (2) Assembly begins when Mdv1p binds the Fis1p TPR-like binding pocket. The NH_2-terminal arm facilitates this interaction but is not strictly required as previously proposed. (3) In the next step, the Fis1p–Mdv1p complex serves as an assembly platform for Dnm1p, which binds as a dimer or a preassembled oligomer. This differs from previous models, which propose that Dnm1p membrane recruitment is the first step in complex assembly. Cyt, cytoplasm; OM, mitochondrial outer membrane; IMS, inter membrane space.

Mechanism of Fis1-3p suppression by $Mdv1^{E250G}$p

What molecular changes are caused by *fis1-3* mutations, and how are these overcome by $Mdv1^{E250G}$p? We show that the Fis1-3p–binding pocket mutations increase the overall flexibility and protease sensitivity of the protein fold. However, the mutant protein can fold in vitro, is expressed and targeted to mitochondria at levels similar to wild type in vivo, and is rescued by the $Mdv1^{E250G}$ suppressor protein. We propose that the mutant protein fold resembles wild type but is more flexible at elevated temperatures. This increased flexibility weakens the interaction between the Fis1p TPR-like pocket and its binding partners, abolishing stable fission complex assembly. The E250G suppressor mutation stabilizes Fis1-3–$Mdv1^{E250G}$p interactions, and these stabilized complexes efficiently recruit Dnm1p to form functional fission complexes.

Three different assays indicate that fission complex stabilization results from increased affinity of $Mdv1^{E250G}$p for Fis1-3p. First, GFP-$Mdv1^{E250G}$p localizes to Fis1-3p–containing mitochondria more efficiently than wild-type GFP-Mdv1p. Second, significantly more $Mdv1^{E250G}$p coimmunoprecipitates with Fis1p and Fis1-3p compared with wild-type Mdv1p. Third, Mdv1p interaction with Fis1-3p is restored by the Mdv1p E250G mutation in yeast two-hybrid assays. Importantly, the $Mdv1^{E250G}$ suppressor protein primarily affects Mdv1p–Fis1p interactions; in two-hybrid assays, Mdv1p–Mdv1p and Mdv1p–Dnm1p interactions are unaffected by this suppressor mutation.

Despite its increased interaction with both wild-type Fis1p and Fis1-3p (Fig. 5 B), $Mdv1^{E250G}$p does not cause fission defects in cells expressing wild-type Fis1p. Thus, enhanced binding between Mdv1p and Fis1p does not appear to interfere with downstream events in fission. One possible interpretation of this result is that dissociation of Mdv1p from Fis1p is not required for late steps in fission.

Although the $Mdv1^{E250G}$p suppressor increases interactions with Fis1-3p, the suppression is not allele specific. $Mdv1^{E250G}$p also rescues other conditional *fis1* alleles contain-

ing TPR domain mutations (unpublished data). Moreover, two additional *MDV1* alleles containing mutations in or near the predicted coiled coil suppress fission defects in *fis1-3* (unpublished data). We propose that different TPR-like binding pocket mutations in Fis1p cause similar structural changes and that these changes are suppressed by a novel class of *MDV1* alleles with mutations in the predicted coiled coil.

Previous work showed that amino acids NH_2-terminal to the Mdv1p coiled coil are sufficient for Fis1p interactions (Tieu et al., 2002). This study also suggested that the coiled-coil region mediates Mdv1p self-interactions. Our studies suggest that Mdv1p suppressor mutations in the predicted coiled-coil region affect Fis1p, but not Mdv1p, interactions. Clearly, the mechanisms regulating Mdv1p–Fis1p interactions in vivo are more complicated than previously appreciated. One possibility is that the Mdv1p coiled coil regulates binding of the Mdv1p NH_2-terminal region to the Fis1p TPR-like domain.

A revised model for assembly of mitochondrial fission complexes

Current models propose that Dnm1p assembles into mitochondrial fission complexes, and Mdv1p recruitment into these complexes activates a rate-limiting step in the fission pathway (Shaw and Nunnari, 2002; Cerveny and Jensen, 2003; Osteryoung and Nunnari, 2003). In our study, Dnm1p assembly defects in *fis1* mutants are rescued by restoring Fis1p interactions with either Mdv1p or Mdv1^{E250G}p. Based on these findings, we favor the idea that direct association of Mdv1p with Fis1p precedes and facilitates Dnm1p recruitment (Fig. 10). According to this revised model, Mdv1p recruitment into fission complexes cannot be rate limiting.

Several other observations are consistent with the idea that Dnm1p assembles onto preexisting Fis1p–Mdv1p complexes. GFP-Mdv1p is constitutively and uniformly bound to Fis1p on the outer membrane as well as in fission complexes with Dnm1p (unpublished data). Thus, it is likely that Dnm1p assembles from the cytoplasm onto Fis1p–Mdv1p complexes. Although Dnm1p assembles into nonfunctional fission complexes in *mdv1*-null cells (Fekkes et al., 2000; Mozdy et al., 2000; Tieu and Nunnari, 2000; Cerveny et al., 2001), we observed that the number, distribution, and size of Dnm1p complexes differ slightly from those in *MDV1* wild-type cells (unpublished data). The latter observation is explained by a recent study showing that Mdv1p and its paralogue Caf4p play redundant roles in Dnm1p recruitment and assembly (Griffin et al., 2005), although only Mdv1p is essential for fission. In the future, it will be important to understand how Dnm1p and Mdv1p are reorganized after assembly to form the functional fission complexes observed in vivo.

Materials and methods

Strain and plasmid construction

Strains used in this study were derived from the FY genetic background (Winston et al., 1995). Standard methods were used for growth, transformation, and genetic manipulation of *S. cerevisiae* (Sherman et al., 1986; Guthrie and Fink, 1991) and *E. coli* (Maniatis et al., 1982). All mutations, disruptions, tag insertions, and replacements were confirmed by PCR, DNA sequencing, and, where appropriate, Western blotting.

To construct pET24a + *fis1* $^{1–127}$10HIS and pET24a + *fis1-3*$^{1–127}$10HIS, *fis1* fragments were PCR amplified with a 3′ 10*HIS* tag encoded by the reverse PCR primer and ligated into NdeI–SalI–digested pET24a(+). To construct pBT + *fis1*$^{1–127}$, a *fis1*$^{1–127}$ PCR fragment flanked by EcoRI–XhoI sites was cloned into pBT to create an in-frame fusion of *FIS1*$^{1–127}$ with the *lambda-cI* gene of the pBT vector backbone. For pTRG + *MDV1*, an *MDV1* PCR fragment flanked by EcoRI–XhoI sites was first cloned into pBT and then subcloned into pTRG using NotI–XhoI sites to create an in-frame fusion with the *RNAPα* gene of the pTRG vector backbone. All inserts used for yeast two-hybrid assays were PCR amplified and cloned into BamH1–SalI–digested pAD-C1 and pBD-C1 (James et al., 1996). To construct pRS415*MET25* + 9*MYC-FIS1* and pRS415*MET25* + 9*MYC–fis1-3*, PCR-amplified fragments flanked by HindIII–XhoI sites were cloned into pRS415*MET25-9MYC* (Mozdy et al., 2000). For pRS416*MET25* + *MDV1* and pRS416*MET25* + *mdv1*^{E250G}, pRS415*MET25* + *fis1*$^{15–155}$, PCR fragments were cloned into BamHI–SalI–digested vector backbones. pRS415*MET25* + *GFP-mdv1*^{E250G} was created by site-directed mutagenesis (Stratagene) using pRS415*MET25* + *GFP-MDV1* as a template. To construct pRS415*MET25* + *GFP-MDV1* and pRS416*MET25* + *GFP-MDV1*, *MDV1* PCR fragments flanked by SalI–XhoI sites were cloned into pRS415*MET25* + *GFP* or pRS416*MET25* + *GFP* plasmids.

Selection and integration of *fis1-ts* alleles

Mutations introduced into the *FIS1* ORF by PCR amplification with Taq DNA polymerase were ligated into linearized pRS416 by in vivo gap repair (Orr-Weaver et al., 1983) in *fis1Δ fzo1Δ* cells. Cells containing *fis1-ts* plasmids were identified by their ability to grow on glycerol at 37°C, but not 25°C. After recovery and phenotypic verification, plasmids were sequenced to identify mutations in the *FIS1* ORF. Mutations in alleles with multiple amino acid changes were separated by site-directed mutagenesis, and only mutations contributing to the phenotype were analyzed further. *fis1-ts* alleles were integrated into the *FIS1* locus using a two-step replacement scheme. First, the *FIS1* ORF was replaced with *URA3* by standard homologous recombination techniques (Rothstein, 1991). Second, *URA3* was replaced with a *fis1-ts* allele by homologous recombination, an event detected by selection on medium containing 5FOA (Boeke et al., 1987). Putative *fis1-ts* integrants were screened by PCR and confirmed by DNA sequencing.

Screen for mdv1 suppressors of *fis1-ts* alleles

mdv1 suppressors of *fis1-ts* alleles were generated by PCR mutagenesis and gap repair as described for selection of *fis1-ts* alleles, except that mutations were introduced into the *MDV1* ORF by gap repair with linearized pRS415-*MET25* in the *fis1-ts fzo1-1* strain. *fis1-ts fzo1-1* cells containing *mdv1* suppressor mutations on plasmids were no longer able to grow on glycerol at 37°C.

Bacterial and yeast two-hybrid analyses

Yeast two-hybrid studies were performed in the Y187 *S. cerevisiae* strain background (CLONTECH Laboratories, Inc.) via a filter-lift assay as described previously (Guthrie and Fink, 2002).

The *E. coli* BacterioMatch II Two Hybrid System (Stratagene) was used to evaluate direct interactions of proteins expressed from the pBT + *fis1*$^{1–127}$ and pTRG + *MDV1* plasmids. Interaction between proteins was assayed by spotting serial dilutions (1:5) of cells on M9 − histidine + 8 μg/ml tetracycline, 25 μg/ml chloramphenicol, and 0.05 mM IPTG in the presence and absence of 5 mM 3AT (Sigma-Aldrich) and monitoring growth at 30°C after 2 d.

Fluorescence microscopy and quantification of mitochondrial phenotypes

Mitochondrial morphology was scored in wild-type and mutant cells expressing fast-folding mitochondrial-targeted red fluorescent protein (mt-RFP; provided by B. Glick, University of Chicago, Chicago, IL; Bevis and Glick, 2002) from pYX142 (Novagen), pRS414-GPD (Mumberg et al., 1995), or pRS416-GPD (Mumberg et al., 1995) plasmids. Dnm1-GFP localization was scored in strains expressing both Dnm1p-rsGFP (Mozdy et al., 2000) from pRS414 or pRS416 and mt-RFP. GFP-Mdv1p localization was scored in strains expressing both GFP-Mdv1p from pRS415-*MET25* or pRS416*MET25* and mt-RFP. Basal levels of GFP-Mdv1p transcription from the *MET25* promoter without induction produced sufficient GFP-Mdv1p (a two- to fivefold increase over endogenous Mdv1p levels) for visualization with no adverse affects on mitochondrial morphology or fission protein localization.

Before quantification, strains were grown overnight at 25°C, diluted to 0.5 OD_{600}, split into 37 and 25°C cultures, and grown another 2–3 h into log phase. Strains overexpressing genes from the *MET25* pro-

moter were induced for either 2 h or 30 min. For 2-h inductions, strains were diluted to 0.5 OD_{600} in medium lacking methionine. Strains induced for 30 min were grown for 1.5 h after dilution, resuspended in medium lacking methionine, and grown another 30 min into log phase. In log phase cultures under repressed conditions, the *MET25* promoter is leaky and produces two- to fivefold more Mdv1p or $Mdv1^{E250G}$p than the endogenous *MDV1* promoter. After induction for 30 min to 2 h, production of Mdv1p or $Mdv1^{E250G}$p by the *MET25* promoter increased to ~50-fold endogenous levels.

Cells were visualized using a microscope (Axioplan 2 Imaging; Carl Zeiss MicroImaging, Inc.) equipped with differential interference contrast (DIC) optics, epifluorescence capabilities, and a Plan-Apochromat × 100 objective (NA 1.4; Carl Zeiss MicroImaging, Inc.). Filter sets (excitation/beamsplitter/emission) for GFP and red fluorescent protein fluorescence were BP 470 ± 20/FT 495/LP 525 ± 25 and BP 546 ± 6/FT 560/BP 575–640, respectively. Images were captured and deconvolved using a monochrome digital camera (AxioCam; Carl Zeiss MicroImaging, Inc.) and appropriate software (AxioVision 3.1; Carl Zeiss MicroImaging, Inc.) and were assembled using Photoshop (Adobe Systems).

Protein purification and limited proteolysis

BL21(DE3) *E. coli* cells (Novagen) containing either pET24a + $fis1^{1–127}$ 10HIS or pET24a + $fis1\text{-}3^{1–127}$10HIS plasmids were grown in LB medium plus 30 μg/ml of kanamycin at 37°C to mid-log phase and induced with 1 mM IPTG for 2–4 h. Cells expressing $Fis1^{1–127}$10Hisp were induced at 37°C, and cells expressing Fis1-$3^{1–127}$10Hisp were induced at RT. Wild-type and mutant Fis1 fusion proteins were purified from cleared cell lysates on Ni^{2+} affinity column chromatography as described by the manufacturer (Novagen).

Limited proteolysis of purified $Fis1^{1–127}$10Hisp and Fis1-$3^{1–127}$10Hisp proteins was performed by incubating 1 or 1.8 μg, respectively, in buffer (100 mM NaCl, 20 mM sodium phosphate, pH 7.0, 1 mM DTT, and 100 μM EDTA) with either 0, 0.1, 0.5, 1.0, 2.0, 3.0, 4.0, or 5.0 μg of trypsin (Sigma-Aldrich) in a 10-μl reaction volume. Reactions were prepared on ice, incubated for 2 min at 37°C, and stopped by boiling in 5× SDS-PAGE sample buffer. Samples were analyzed by SDS-PAGE and Western blotting using anti-Fis1p antibodies (Mozdy et al., 2000). For mass spectrometry analysis, purified proteins were dialyzed in buffer (150 mM NaCl, 20 mM sodium phosphate buffer, pH 7.0, and 25 mM DTT), and 9.5 μM of either $Fis1^{1–127}$10Hisp or Fis1-$3^{1–127}$10Hisp was digested with 4 μg of trypsin for 2 min at 37°C. Reactions were stopped with 1% trifluoroacetic acid at RT and then frozen at −80°C until analysis. Samples were analyzed by electrospray ionization at the University of Utah Mass Spectrometry Facility.

CoIP assays

CoIP assays were performed using *mdv1Δ* strains expressing Fis1p, 9Myc-Fis1p, or 9Myc–Fis1-3p from the genomic locus and either pRS416-*MET25-MDV1* or pRS416-*MET25-*$mdv1^{E250G}$ from a plasmid. For Dnm1p–Fis1p coIPs with DSP cross-linking, strains were grown at 25°C in synthetic dextrose medium to early log phase, washed, resuspended in medium lacking methionine, and grown at 37°C for another hour. A total of 35 OD_{600} units of cells were collected. Cells were treated as described previously for mitochondrial preparation (Kondo-Okamoto et al., 2003) with the following modifications. After Zymolyase treatment for 45 min at 37°C, cross-linking was performed with 2.5 mM DSP (Pierce Chemical Co.) for an additional 30 min, and DSP was quenched by addition of 50 mM glycine (also present in all subsequent buffers). After homogenization, samples were used directly for coIP without mitochondrial isolation. Homogenized samples were solubilized for 15 min in IP buffer (1% Triton X-100, 150 mM NaCl, 30 mM Hepes-KOH, pH 7.4, and 1:500 protease inhibitor cocktail [Calbiochem]). After centrifugation at 12,500 *g* for 10 min, the supernatant was incubated with 40 μl anti–c-Myc agarose-conjugated beads (Sigma-Aldrich) for 1 h at 4°C. Agarose beads were collected, washed in IP buffer, and incubated in 50 μl SDS-PAGE sample buffer lacking β-mercaptoethanol at 60°C for 8 min to release bound proteins. After addition of β-mercaptoethanol and boiling, samples were analyzed by SDS-PAGE and Western blotting with anti-Myc (Santa Cruz Biotechnology, Inc.), affinity-purified anti-Dnm1p (Otsuga et al., 1998), and anti-porin (Invitrogen) antibodies. The load was 0.7 OD_{600} cell equivalents per lane, and the elution was 34 OD_{600} cell equivalents per lane.

For coIP without DSP cross-linking, cells were grown overnight at 25°C in S-dextrose lacking leucine and diluted to 0.5 OD_{600} in S-dextrose lacking leucine and methionine at 37°C, and 70 OD_{600} cells were harvested. CoIP was performed as described previously (Fukushima et al., 2001) with the following changes: lysis was performed in IP buffer (0.5% Triton, 150 mM NaCl, 1 mM EDTA, 50 mM Tris, pH 7.4, and 1:500 protease inhibitor cocktail set III [Calbiochem]), and soluble proteins were precipitated with anti-Myc beads at 4°C for 2 h. Proteins were eluted and analyzed as described in the previous paragraph, decorating with anti-Mdv1p (provided by J. Nunnari, University of California, Davis, Davis, CA), anti-Myc, and anti-porin antibodies. The load was 1.25 OD_{600} cell equivalents per lane, and the elution was 21 OD_{600} cell equivalents per lane.

Online supplemental material

Fig. S1 shows that $Mdv1^{E250G}$p behaves like wild-type Mdv1p in the presence of wild-type Fis1p. Online supplemental material is available at http://www.jcb.org/cgi/content/full/jcb.200506158/DC1.

We greatly appreciate discussions with all members of the Shaw Laboratory. We also thank D. Bhar, M. Babst, and members of B. Graves' laboratory for stimulating discussions and technical assistance and C. Nelson (University of Utah's Health Sciences Center Core Facility for Mass Spectrometry and Proteomics, Salt Lake City, Utah) for performing mass spectrometry experiments. We thank B. Glick for providing a plasmid-encoding FastFold DsRed (mt-RFP) and J. Nunnari for providing the anti-Mdv1p antibody.

This work was funded by a National Institutes of Health (NIH) grant awarded to J.M. Shaw (GM53466), an NIH training grant awarded to E.M. Coonrod (5 T32 DK007115), and a University of Utah Bioscience Undergraduate Research Program grant awarded to T.K. Anderson. The Utah Health Sciences DNA/Peptide and Sequencing Facilities are supported by a National Cancer Institute grant (5-P30CA42014).

Submitted: 24 June 2005
Accepted: 19 September 2005

References

Arimura, S., and N. Tsutsumi. 2002. A dynamin-like protein (ADL2b), rather than FtsZ, is involved in *Arabidopsis* mitochondrial division. *Proc. Natl. Acad. Sci. USA.* 99:5727–5731.

Bevis, B.J., and B.S. Glick. 2002. Rapidly maturing variants of the *Discosoma* red fluorescent protein (DsRed). *Nat. Biotechnol.* 20:83–87.

Bleazard, W., J.M. McCaffery, E.J. King, S. Bale, A. Mozdy, Q. Tieu, J. Nunnari, and J.M. Shaw. 1999. The dynamin-related GTPase Dnm1 regulates mitochondrial fission in yeast. *Nat. Cell Biol.* 1:298–304.

Boeke, J.D., J. Trueheart, G. Natsoulis, and G.R. Fink. 1987. 5-Fluoroorotic acid as a selective agent in yeast molecular genetics. *Methods Enzymol.* 154:164–175.

Bossy-Wetzel, E., M.J. Barsoum, A. Godzik, R. Schwarzenbacher, and S.A. Lipton. 2003. Mitochondrial fission in apoptosis, neurodegeneration and aging. *Curr. Opin. Cell Biol.* 15:706–716.

Cerveny, K.L., and R.E. Jensen. 2003. The WD-repeats of Net2p interact with Dnm1p and Fis1p to regulate division of mitochondria. *Mol. Biol. Cell.* 14:4126–4139.

Cerveny, K.L., J.M. McCaffery, and R.E. Jensen. 2001. Division of mitochondria requires a novel DNM1-interacting protein, Net2p. *Mol. Biol. Cell.* 12:309–321.

Chen, H., and D.C. Chan. 2004. Mitochondrial dynamics in mammals. *Curr. Top. Dev. Biol.* 59:119–144.

D'Andrea, L.D., and L. Regan. 2003. TPR proteins: the versatile helix. *Trends Biochem. Sci.* 28:655–662.

Dohm, J.A., S.J. Lee, J.M. Hardwick, R.B. Hill, and A.G. Gittis. 2004. Cytosolic domain of the human mitochondrial fission protein fis1 adopts a TPR fold. *Proteins.* 54:153–156.

Fekkes, P., K.A. Shepard, and M.P. Yaffe. 2000. Gag3p, an outer membrane protein required for fission of mitochondrial tubules. *J. Cell Biol.* 151: 333–340.

Frank, S., B. Gaume, E.S. Bergmann-Leitner, W.W. Leitner, E.G. Robert, F. Catez, C.L. Smith, and R.J. Youle. 2001. The role of dynamin-related protein 1, a mediator of mitochondrial fission, in apoptosis. *Dev. Cell.* 1:515–525.

Fukushima, N.H., E. Brisch, B.R. Keegan, W. Bleazard, and J.M. Shaw. 2001. The GTPase effector domain sequence of the Dnm1p GTPase regulates self-assembly and controls a rate-limiting step in mitochondrial fission. *Mol. Biol. Cell.* 12:2756–2766.

Griffin, E.E., J. Graumann, and D.C. Chan. 2005. The WD40 protein Caf4p is a component of the mitochondrial fission machinery and recruits Dnm1p to mitochondria. *J. Cell Biol.* 170:237–248.

Guthrie, C., and G. Fink. 1991. *Guide to yeast genetics and molecular biology.* Methods in Enzymology. Vol. 194. San Diego: Academic Press, Inc.

Guthrie, C., and G. Fink. 2002. *Guide to yeast genetics and molecular biology.* Methods in Enzymology. Vol. 350. San Diego: Academic Press, Inc.

Hales, K.G., and M.T. Fuller. 1997. Developmentally regulated mitochondrial fusion mediated by a conserved, novel, predicted GTPase. *Cell.* 90:121–129.

Hermann, G.J., and J.M. Shaw. 1998. Mitochondrial dynamics in yeast. *Annu. Rev. Cell Dev. Biol.* 14:265–303.

Hermann, G.J., J.W. Thatcher, J.P. Mills, K.G. Hales, M.T. Fuller, J. Nunnari, and J.M. Shaw. 1998. Mitochondrial fusion in yeast requires the transmembrane GTPase Fzo1p. *J. Cell Biol.* 143:359–373.

Holm, L., and C. Sander. 1993. Protein structure comparison by alignment of distance matrices. *J. Mol. Biol.* 233:123–138.

Jagasia, R., P. Grote, B. Westermann, and B. Conradt. 2005. DRP-1-mediated mitochondrial fragmentation during EGL-1-induced cell death in *C. elegans*. *Nature.* 433:754–760.

James, D.I., P.A. Parone, Y. Mattenberger, and J.C. Martinou. 2003. hFis1, a novel component of the mammalian mitochondrial fission machinery. *J. Biol. Chem.* 278:36373–36379.

James, P., J. Halladay, and E.A. Craig. 1996. Genomic libraries and a host strain designed for highly efficient two-hybrid selection in yeast. *Genetics.* 144:1425–1436.

Jensen, R.E., A.E. Hobbs, K.L. Cerveny, and H. Sesaki. 2000. Yeast mitochondrial dynamics: fusion, division, segregation, and shape. *Microsc. Res. Tech.* 51:573–583.

Karbowski, M., and R.J. Youle. 2003. Dynamics of mitochondrial morphology in healthy cells and during apoptosis. *Cell Death Differ.* 10:870–880.

Kondo-Okamoto, N., J.M. Shaw, and K. Okamoto. 2003. Mmm1p spans both the outer and inner mitochondrial membranes and contains distinct domains for targeting and foci formation. *J. Biol. Chem.* 278:48997–49005.

Labrousse, A.M., M.D. Zappaterra, D.A. Rube, and A.M. van der Bliek. 1999. *C. elegans* dynamin-related protein DRP-1 controls severing of the mitochondrial outer membrane. *Mol. Cell.* 4:815–826.

Lee, Y.J., S.Y. Jeong, M. Karbowski, C.L. Smith, and R.J. Youle. 2004. Roles of the mammalian mitochondrial fission and fusion mediators Fis1, Drp1, and Opa1 in apoptosis. *Mol. Biol. Cell.* 15:5001–5011.

Legesse-Miller, A., R.H. Massol, and T. Kirchhausen. 2003. Constriction and Dnm1p recruitment are distinct processes in mitochondrial fission. *Mol. Biol. Cell.* 14:1953–1963.

Li, Z., K. Okamoto, Y. Hayashi, and M. Sheng. 2004. The importance of dendritic mitochondria in the morphogenesis and plasticity of spines and synapses. *Cell.* 119:873–887.

Maniatis, T., E.F. Fritsch, and J. Sambrook. 1982. Molecular Cloning: A Laboratory Manual. Cold Spring Harbor Laboratory, Cold Spring Harbor, NY. 545 pp.

Mozdy, A.D., and J.M. Shaw. 2003. A fuzzy mitochondrial fusion apparatus comes into focus. *Nat. Rev. Mol. Cell Biol.* 4:468–478.

Mozdy, A.D., J.M. McCaffery, and J.M. Shaw. 2000. Dnm1p GTPase-mediated mitochondrial fission is a multi-step process requiring the novel integral membrane component Fis1p. *J. Cell Biol.* 151:367–380.

Mumberg, D., R. Muller, and M. Funk. 1995. Yeast vectors for the controlled expression of heterologous proteins in different genetic backgrounds. *Gene.* 156:119–122.

Okamoto, K., and J.M. Shaw. 2005. Mitochondrial morphology and dynamics in yeast and multicellular eukaryotes. *Annu. Rev. Genet.* 39:503–536.

Orr-Weaver, T.L., J.W. Szostak, and R.J. Rothstein. 1983. Genetic applications of yeast transformation with linear and gapped plasmids. *Methods Enzymol.* 101:228–245.

Osteryoung, K.W., and J. Nunnari. 2003. The division of endosymbiotic organelles. *Science.* 302:1698–1704.

Otsuga, D., B.R. Keegan, E. Brisch, J.W. Thatcher, G.J. Hermann, W. Bleazard, and J.M. Shaw. 1998. The dynamin-related GTPase, Dnm1p, controls mitochondrial morphology in yeast. *J. Cell Biol.* 143:333–349.

Rapaport, D., M. Brunner, W. Neupert, and B. Westermann. 1998. Fzo1p is a mitochondrial outer membrane protein essential for the biogenesis of functional mitochondria in *Saccharomyces cerevisiae*. *J. Biol. Chem.* 273:20150–20155.

Rothstein, R. 1991. Targeting, disruption, replacement, and allele rescue: integrative DNA transformation in yeast. *Methods Enzymol.* 194:281–301.

Scorrano, L. 2003. Divide et impera: Ca^{2+} signals, mitochondrial fission and sensitization to apoptosis. *Cell Death Differ.* 10:1287–1289.

Sesaki, H., and R.E. Jensen. 1999. Division versus fusion: Dnm1p and Fzo1p antagonistically regulate mitochondrial shape. *J. Cell Biol.* 147:699–706.

Shaw, J.M., and J. Nunnari. 2002. Mitochondrial dynamics and division in budding yeast. *Trends Cell Biol.* 12:178–184.

Sherman, F., G.R. Fink, and J.B. Hicks. 1986. Methods in Yeast Genetics. Cold Spring Harbor Laboratory Press, Cold Spring Harbor, NY. 186 pp.

Smirnova, E., D.L. Shurland, S.N. Ryazantsev, and A.M. van der Bliek. 1998. A human dynamin-related protein controls the distribution of mitochondria. *J. Cell Biol.* 143:351–358.

Stojanovski, D., O.S. Koutsopoulos, K. Okamoto, and M.T. Ryan. 2004. Levels of human Fis1 at the mitochondrial outer membrane regulate mitochondrial morphology. *J. Cell Sci.* 117:1201–1210.

Suzuki, M., S.Y. Jeong, M. Karbowski, R.J. Youle, and N. Tjandra. 2003. The solution structure of human mitochondria fission protein Fis1 reveals a novel TPR-like helix bundle. *J. Mol. Biol.* 334:445–458.

Suzuki, M., A. Neutzner, N. Tjandra, and R.J. Youle. 2005. Novel structure of the N terminus in yeast Fis1 correlates with a specialized function in mitochondrial fission. *J. Biol. Chem.* 280:21444–21452.

Szabadkai, G., A.M. Simoni, M. Chami, M.R. Wieckowski, R.J. Youle, and R. Rizzuto. 2004. Drp-1-dependent division of the mitochondrial network blocks intraorganellar Ca^{2+} waves and protects against Ca^{2+}-mediated apoptosis. *Mol. Cell.* 16:59–68.

Tieu, Q., and J. Nunnari. 2000. Mdv1p is a WD repeat protein that interacts with the dynamin-related GTPase, Dnm1p, to trigger mitochondrial division. *J. Cell Biol.* 151:353–366.

Tieu, Q., V. Okreglak, K. Naylor, and J. Nunnari. 2002. The WD repeat protein, Mdv1p, functions as a molecular adaptor by interacting with Dnm1p and Fis1p during mitochondrial fission. *J. Cell Biol.* 158:445–452.

van der Bliek, A.M. 2000. A mitochondrial division apparatus takes shape. *J. Cell Biol.* 151:F1–F4.

Westermann, B. 2002. Merging mitochondria matters: cellular role and molecular machinery of mitochondrial fusion. *EMBO Rep.* 3:527–531.

Westermann, B. 2003. Mitochondrial membrane fusion. *Biochim. Biophys. Acta.* 1641:195–202.

Westermann, B., and H. Prokisch. 2002. Mitochondrial dynamics in filamentous fungi. *Fungal Genet. Biol.* 36:91–97.

Winston, F., C. Dollard, and S.L. Ricupero-Hovasse. 1995. Construction of a set of convenient *Saccharomyces cerevisiae* strains that are isogenic to S288C. *Yeast.* 11:53–55.

Yaffe, M.P. 1999. The machinery of mitochondrial inheritance and behavior. *Science.* 283:1493–1497.

Yoon, Y., E.W. Krueger, B.J. Oswald, and M.A. McNiven. 2003. The mitochondrial protein hFis1 regulates mitochondrial fission in mammalian cells through an interaction with the dynamin-like protein DLP1. *Mol. Cell. Biol.* 23:5409–5420.